

The extraplanar stellar populations of highly-inclined disk galaxies IC 2233, IC 5052, NGC 4631 and NGC 5023 are analyzed with the goal to quantify their vertical extent and structure. Based on the single-star photometry, we separate different stellar populations and analyze their spatial distribution. On archival images obtained with the Hubble Space Telescope ACS/WFC the surroundings of these galaxies are well resolved into stars with the red giant population (RGB) identified far above the galaxy mid-planes. We find that there are a profound change in slope of the number density profile of the evolved RGB stars at extraplanar height of $4 - 8$ kpc, that possibly reflects a truncation of the thick disk and reaching the $2 - 3$ times more extended oblate stellar component (“the halo”). This structure is consistent with our previous studies of both edge-on and face-on disk galaxies in the Local Universe (Tikhonov et al. 2005a,b) and allow us to improve the spatial model of the stellar components of a typical spiral galaxy. In NGC 4631, the revealed asymmetry of its stellar thick disk and halo, is likely caused by the neighbor dwarf galaxy NGC 4627. Based on the tip of the red giant branch method (TRGB) we estimated a distance of 10.42 ± 0.38 Mpc for IC 2233, 5.62 ± 0.20 Mpc for IC 5052, 7.11 ± 0.13 Mpc for NGC 4631 (6.70 ± 0.15 for its satellite NGC 4627) and 6.14 ± 0.15 Mpc for NGC 5023. We confirm the presence of slight extraplanar metallicity gradient of evolved stars at NGC 5023 and IC 5052, based on the systematic changes of the colour distribution of red giant stars.

Key words. Galaxies: individual: IC 2233, IC 5052, NGC 4631, NGC 4627, NGC 5023 — galaxies: stellar content — galaxies: photometry — galaxies: structure

Stellar halos and thick disks around edge-on spiral galaxies IC 2233, IC 5052, NGC 4631 and NGC 5023. *

Tikhonov N.A.^{1,2}, Galazutdinova O.A.^{1,2}, Drozdovsky I.O.^{3,4}

¹ Special Astrophysical Observatory, Russian Academy of Sciences, N.Arkhyz, KChR,
369167, Russia

² Isaac Newton Institute of Chile, SAO Branch, Russia

³ Instituto de Astrofísica de Canarias, E-38200, Tenerife, Spain

⁴ Astronomical Institute, St.Petersburg University, 198504, Russia

Received January 30, 2006; accepted

Abstract.

1. Introduction

Understanding the structure of the stellar component of disk galaxies is an important step for unraveling their formation and evolution. Although challenging to measure, the extraplanar stellar content around galaxies is a potentially-important probe of the most ancient stellar populations, as well as of the role of that different external and internal processes play in the evolution of modern galaxies, such as: merging, accretion and infall of metal-poor gas and satellite galaxies (e.g., Abadi et al. 2003; Brook et al. 2004; Bullock & Johnson 2005); disk heating (e.g., Kroupa 2002; Gnedin 2003); or the ejection of gas from the underlying disk, which may cool so that stars can form (e.g., Howk & Savage 1999; Savage et al. 2003).

The stellar outskirts around our own Galaxy and some other large spiral galaxies has been extensively studied over the last few years and revealed faint stellar envelopes in many of them (e.g., Sackett 1999; Cuillandre et al. 1999; van der Marel 2002; Ferguson et al. 2002; Dalcanton & Bernstein 2002; Zibetti & Ferguson 2004). The most extensive and detailed study of the outer stellar populations of the Milky Way and M 31 revealed complex patchy structures with numerous streams, which appear to be the remnants of disrupted companion galaxies

* Based on observations with the NASA/ESA Hubble Space Telescope, obtained at the Space Telescope Science Institute, which is operated by the Association of Universities for Research in Astronomy, Inc., under NASA contract NAS 5-26555.

(e.g., Brown et al. 2003; Zucker et al. 2004). However, the chemical patterns of the stars of the dwarf spheroidal (dSph), and irregular (LMC and SMC) satellite galaxies are predominantly distinct from the stars in each of the kinematic components of the Galaxy. This result rules out continuous merging of low-mass galaxies similar to the currently observed satellites during the formation of the Milky Way (e.g., Smecker-Hane et al. 1998; McWilliam & Smecker-Hane 2005; Venn et al. 2004). At the same time, the detection of extraplanar cold and ionized gas regions at large distances from the mid-planes of some spiral galaxies, which must be powered by hot stars, suggests that while most of the outer, elusive stellar components are predominantly evolved, some fraction of these stars are not a single burst ancient stellar population (e.g., Keppel et al. 1991; Hoopes et al. 1999; Howk & Savage 1999; Tüllmann et al. 2003).

In the literature, the definition “halo” and “thick disk” is rather unclear, as well as the method of their separation are not well established yet. While some of the recent studies of the outer regions of spiral galaxies rely on multicolour surface photometry, successful detection is only possible in the deep observations of the edge-on galaxies with a prominent thick disk and halo (Dalcanton & Bernstein 2002; Pohlen et al. 2004; Zibetti et al. 2004; Zibetti & Ferguson 2004). For example, Dalcanton & Bernstein (2002) analyzed the sample of 47 edge-on spiral galaxies and have found a presence of the thick disk in 90% of them, based on the results of multi-colour surface photometry. By stacking of 1054 rescaled images of edge-on galaxies in the Sloan DSS Zibetti et al. (2004) detected an extended low surface brightness halo, however the “mean” colours of this component ($g - r = 0.65$ and $r - i = 0.6$) cannot be easily explained by normal stellar populations, and may suggest contamination by ionized gas emission. The important other result obtained at surface photometry studies is that both thin and thick disks are truncated, with mean scaleheight and scalelength of the thick disk is several times larger than that of the thin disk (Pohlen et al. 2004). Given that there have also been some non-detections of luminous thick disk or halo components (e.g Fry et al. 1999; Zheng et al. 1999), the question arises about the ubiquity, origin and further evolution of these outer structures.

The alternative technique of tracking out resolved stars to explore various galactic subsystems sidesteps the difficulties inherent in quantifying extremely faint diffuse emission. The measurement of single-star metallicity and velocity fields can only be applied to distinguish different stellar components in Milky Way and in a handful of nearest galaxies (Gilmore & Reid 1983; Chiba & Beers 2000; Prochaska et al. 2000; Worthey et al. 2005; Ibata et al. 2005). For the more distant galaxies this information is unavailable, and a set of the model dependent assumptions need to be considered. Aside from the spatial distribution law and kinematics, stars from each of the galactic subsystems (bulge, disks, and halo) share a common star formation history retaining considerable age and chemical information (Vallenari et al. 2000; Prochaska et al. 2000; Chiba & Beers 2000; Sarajedini & Van Duyne 2001; Williams 2002; Brewer & Carney 2004). On the basis of multi-colour single-star photometry, one is able to separate different stellar populations, and suggesting that each of the components has a different dominant stellar population, to constrain their spatial distribution.

Table 1. The ACS/WFC Survey Fields

Galaxy	Region	Date	Band	Exposure	ID	N_{stars}
IC2233	S1	2004-04-29	F814w	2×350	9765	27120
		2004-04-29	F606w	2×338	9765	
NGC4631	S1	2003-08-03	F814w	2×350	9765	115315
		2003-08-03	F606w	2×338	9765	
	S2	2004-06-09	F814w	2×350	9765	108980
		2004-06-09	F606w	2×338	9765	
IC5052	S1	2003-12-13	F814w	2×350	9765	63108
		2003-12-13	F606w	2×338	9765	
NGC5023	S1	2004-07-02	F814w	2×350	9765	49628
		2004-07-02	F606w	2×338	9765	

Inspired by the unparalleled angular resolution and sensitivity of the *HST* WFPC2 and ACS, we began a project to analyze the outermost stellar structure of spiral galaxies. In related works, we have analyzed the spatial distribution and properties of the outer stars in the nearby face-on (M 81 and NGC 300), as well as edge-on (NGC 55, NGC 891, NGC 4144, and NGC 4244) spiral galaxies (Tikhonov et al. 2005; Tikhonov & Galazutdinova 2005). In the most massive of the studied disk galaxies we have found a profound change in slope of the number density profile of the evolved red giant branch (RGB) stars, that likely reflects a truncation of the the thick disk and reaching the pure halo stellar component. The similar change of the number density gradient of RGB stars were also reported for lower mass spiral M 33 (Cuillandre et al. 1999; Rowe et al. 2005), as well as in two massive irregular galaxies: IC 10 (Drozdovsky et al. 2003), and M 82 (Tikhonov 2005). These results strongly support the ubiquitous presence of the truncated thick disks in the majority of disk galaxies, as well as large extend of the stellar outskirts in all directions.

In this paper, we selected four high-inclination nearby disk galaxies for an in-depth study of their extraplanar stellar structure: IC 2233, IC 5052, NGC 4631 and NGC 5023. Our primary objectives are to: (i) quantify the stellar population variations associated with extreme outer substructure, and (ii) derive stringent constraints on the age and metallicity of stars in the far outer disk. The choice of high-inclination galaxies ensures minimal contamination by stars belonging to the dominant galactic disk component, and provides the more robust separation of the thick disk and halo stellar populations.

Fig. 1. The DSS-2 images of the galaxies with the ACS/WFC footprints superposed. The edge of thick disk and halo extent are shown by the ellipses.

2. Observations and stellar photometry

To study the resolved stellar population of galaxies, we obtained ACS/WFC images available in the *HST* archive. Digital Sky Survey images of these galaxies with ACS/WFC footprints are shown in Fig. 1. An interior and exterior ellipses delineate an estimated edges of the thick disk and halo. The observational data are listed in Table 1, where ID is the HST program number and N_{stars} is the number of detected stars. Images were reprocessed through the standard ACS STScI pipeline, CALACS, as described by Pavlovsky et al. (2005). All data have first order bias subtraction, dark subtraction, and bad pixel masking applied. Images are then corrected for the flat-field response. We combined images using a latest version of the `Multidrizzle` pack-

age (Koekemoer et al. 2002), which provides an automated method for distortion-correcting and combining dithered images. `Multidrizzle` also corrects for gain and bias offsets between WFC chips, identifies and removes cosmic rays and cosmetic defects. We generate point-source catalogs from the stacked direct image using an automatic star-finding program `DAOPHOT/FIND` in `MIDAS` (Stetson 1994), applying a 3.0σ per pixel detection threshold. The measurements of their magnitudes were conducted via point-spread-function (PSF) fitting that is constructed from the isolated 'PSF-stars' as it is implemented in `DAOPHOT/ALLSTAR`. The background galaxies, unresolved blends and stars contaminated by cosmetic CCD blemishes were eliminated from the final lists, using their peculiar `ALLSTAR` characteristics, $|SHARP| > 0.3$, $\chi > 1.3$ (Stetson 1994). We derived an aperture correction from the 2.5 to the 10 pixels ($0''.5$) aperture radius by analyzing profile of the PSF-stars.

The $F606W$ and $F814W$ instrumental magnitudes have been transformed to standard magnitudes in the Kron-Cousins system adopting our empirically-derived transformation:

$$\begin{aligned} (V - I) &= 1.321 \cdot (v - i) + 1.133 \\ I &= i + 0.059 \cdot (V - I) + 25.972 \end{aligned} \quad (1)$$

These transformations have been calculated using the photometry of 60 stars with $0 < (V - I) < 5.0$, detected in both, ACS/WFC and WFPC2 images of irregular galaxy IC 10, and the prescriptions of Holtzman et al. (1995) for the WFPC2 data. The photometric uncertainties of this calibration are dominated by the accuracy of the PSF-photometry of these stars with a median value of $0.^m03$ in I -band and $0.^m04$ in V .

In Tikhonov et al. (2005) and Tikhonov & Galazutdinova (2005) we applied these equations to the single-star photometry of the ACS/WFC images of NGC 55 and NGC 4244. Based on the derived magnitude of the tip of the red giant branch method, we estimated distances to these galaxies, which agree well with measurements obtained with WFPC2 and other instruments.

With the extinction law of Cardelli et al. (1989) we correct all the photometry for Galactic extinction, adopting the foreground extinction of Schlegel et al. (1998), and assuming that internal extinction in all galaxies is negligible in their outer ("halo") parts.

3. Results

3.1. CM diagrams

The results of photometry for all stars detected in the galaxies are presented as colour-magnitude diagrams (CMD) in the Fig. 2, while Fig. 3 show the CMDs of the stars from the outermost extraplanar areas¹. The features of these diagrams resemble those of spiral galaxies. All the CMDs are characterized by a noticeable red plume, while strength of the blue plume varies a lot. The spatial variations are apparent from the varying strengths of the blue and red plumes, and

¹ Note, that outer part of NGC 4631 also contain some of the stars of the satellite dwarf Sph/Irr galaxy NGC 4627, that are shown on the separate plot

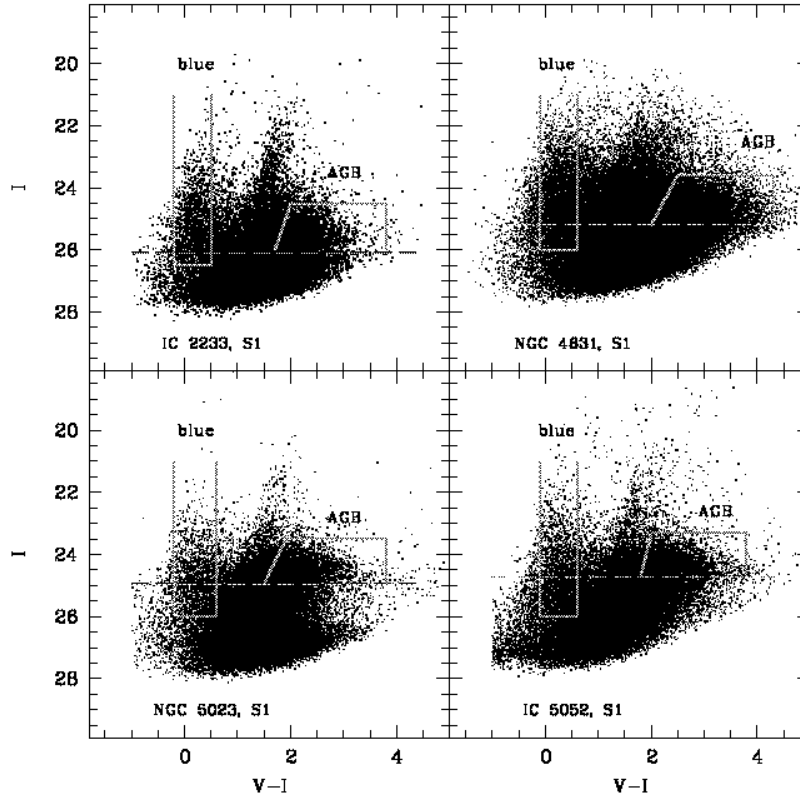


Fig. 2. The $[(V - I), I]$ color-magnitude diagram of all stars located in the ACS/WFC fields of the galaxies. The dashed line shows the position of the TRGB and the solid lines show the regions of the “blue”, and AGB stars.

show systematic dependence from extraplanar distance. The CMDs of the inner-disk areas show a plethora of blue and red supergiants, main-sequence stars, and blue-loop stars. The outermost extraplanar stellar populations are dominated by the old stars of the red giant branch. The dashed line indicates the position of TRGB (the tip of the red giant branch) and above TRGB some of the stars are asymptotic giant branch (AGB) and red supergiant (RSG) stars.

One of the ACS/WFC fields around NGC 4631, additionally includes some stars of the neighboring NGC 4627. Relying on their similar radial velocities Holmberg (1937) included NGC 4631/NGC 4627 in his catalog as a galaxy pair Holmberg 442, while Arp (1966) added them in his catalog of peculiar galaxies as Arp 281. The dwarf companion NGC 4627 is usually classified as dwarf elliptical E4,pec (NED). The increasing overdensity of the stars that lean towards NGC 4627 allow us to separate them from the NGC 4631 thick disk and halo, and examine their appearance in the CMD presented in Fig. 3. The RGB and AGB stars show a well noticeable feature, that complemented by some main-sequence stars at $-0.4 < (V - I) < 0.3$ and $26 < I < 26$, and by a few blue supergiant candidates. If even a small part of these blue young stars belongs to NGC 4627, the classification of this galaxy should be altered to a transitional dSph/Irr type. The relatively blue colour of NGC 4627 ($B - V = 0.62$ (RC3), and clear evidence

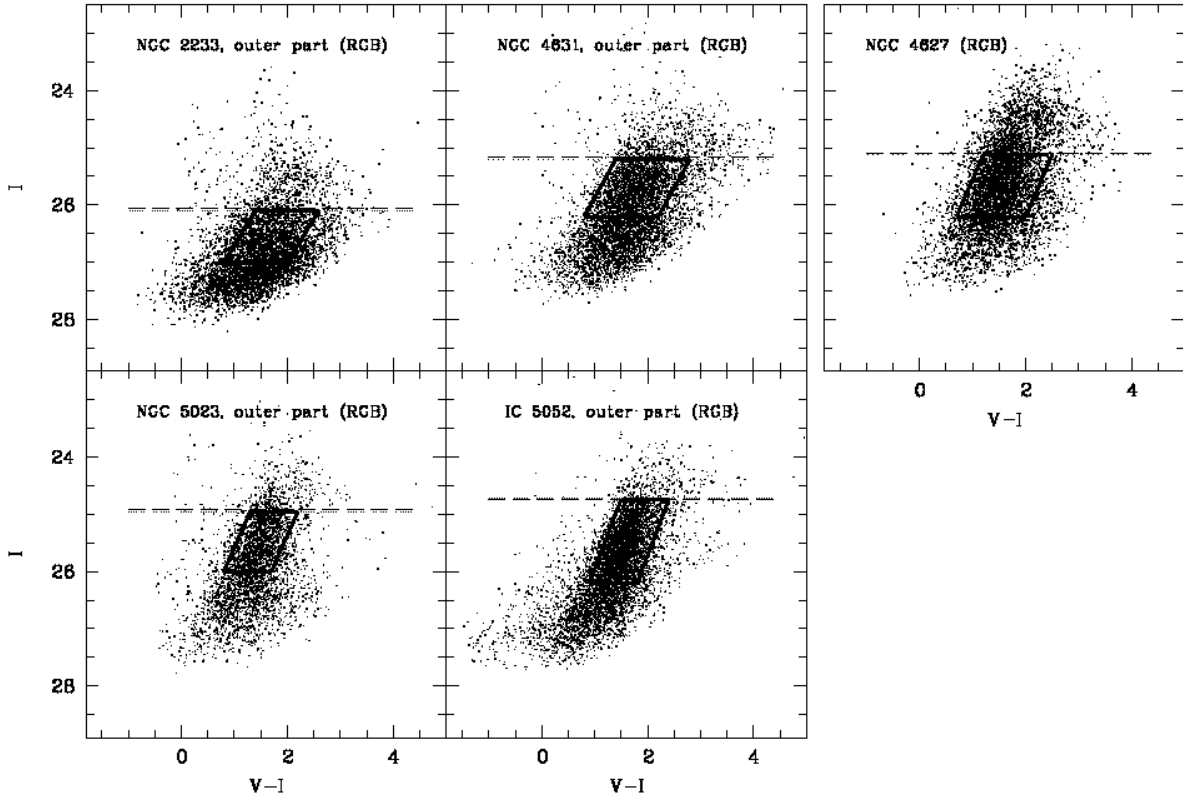


Fig. 3. The $[(V - I), I]$ color-magnitude diagram of the stars located above the thin disk of the galaxies. The dashed line shows the position of the TRGB and the solid lines show the region of the RGB stars.

of the O II-emission around its circumnuclear area (Bettoni & Buson 1987) are also indicative of the current presence of some star formation in this galaxy.

For our spatial structure analysis we used only the stars with magnitudes above the 50% completeness level (i.e. the magnitude where only half the simulated stars are identified), that occurs at about $27.3 \leq I \leq 27.5$ above the limiting $I \sim 28$ mag in these diagrams.

3.2. Distances

The high quality of the presented data provides a valuable opportunity to estimate distances of investigated galaxies, based on one the most successful and reliable distance candle, the luminosity of the TRGB (Lee et al. 1993). While being affected by contamination of bright asymptotic giant branch (AGB) stars, statistical (Poisson) noise of star counts, and dependence from the metallicity/age of RGB stars, the TRGB method gives an estimate of distance with precision and accuracy similar to that of the Cepheids method, $\leq 10\%$ (Lee et al. 1993; Bellazzini et al. 2001).

In order to estimate distances, we have used the outer extraplanar areas in each galaxy, avoiding crowded star formation regions in a thin disk. Since fraction of AGB-to-RGB stars steeply declines with extraplanar distance, we can also expect of decreasing of the contamination by

Fig. 4. Smoothed luminosity function (solid lines) and edge-detection Sobel-filter output (dotted lines) for the red stars. The position of the TRGB corresponds to the peak of the Sobel-filter.

AGB stars in the outermost areas. At the same time, we maintained the coverage large enough to include a statistically significant number of RGB stars. Following the standard technique we calculated the luminosity function of candidate RGB stars, and applied an edge detection algorithm (Sobel filter) to detect the location of the TRGB. The position of the first peak in the convolved function was used to determine the tip magnitude while the width of the peak provides an estimate of the tip error. The stellar luminosity functions and the results of their convolution with Sobel filter are presented in Fig. 4, and reveal a sudden discontinuity which corresponds to the TRGB. Using the method of Lee et al. (1993), we estimate distances to the galaxies and mean metallicity of their red giants. The inferred metallicity of RGB stars should be considered solely as a local value, due to the metallicity gradient commonly seen in spiral galaxies (Tiede et al. 2004). We obtain the following results for the galaxies.

3.2.1. IC 2233

The TRGB in IC 2233 is discerned at $I_{\text{TRGB}} = 26.09 \pm 0.08$, and the median colour of RGB stars $(V - I)_{-3.5,0}$ is $1^m 60$. Using the calibration by Lee et al. (1993), we obtain a metallicity $[\text{Fe}/\text{H}] \approx -0.93$ dex and a distance modulus $(m - M)_0 = 30.09$, corresponding to $D = 10.42 \pm 0.38$ Mpc. Note that the error in distance includes random (residuals in the PSF fitting, tip measurement,

extinction) and systematic (RR Lyrae distance scale, absolute magnitude of TRGB, photometric zero points) uncertainties.

3.2.2. IC 5052

Based on the luminosity function of RGB stars in the outer area of IC 5052 (Fig. 4), the TRGB is at $I_{\text{TRGB},0} = 24.74 \pm 0.07$. The median colour between $I_0 = 25^m 1$ and $I_0 = 25^m 3$, which we use to determine $(V - I)_{-3.5,0}$, is $1^m 66$. These results correspond to a metallicity $[\text{Fe}/\text{H}] \approx -0.9$, and a distance $(m - M)_0 = 28.75$ ($D = 5.62 \pm 0.20$ Mpc).

3.2.3. NGC 4631 & NGC 4627

We have performed single-star photometry for two fields in the vicinity of NGC 4631. One of the fields (S1) partly covers the circumnuclear area of NGC 4631 and the outer part of the satellite dwarf Sph/Irr galaxy NGC 4627, while another area (S2) is at the larger galactocentric distance along the disk plane (see 1). To avoid bright AGB stars of the NGC 4631 disk and bulge, we selected stars of the north-east sector of the S1 field and south part of the S2 field (marked by arrows). The location of the TRGB is found by detecting a sharp edge in the luminosity function of the red plume at $I_{\text{TRGB},0} = 25.20 \pm 0.05$ and median colour of the RGB $(V - I)_{-3.5,0}$ is 1.60 (for stars of S1 field), while for stars of S2 field $I_{\text{TRGB},0}$ is at 25.17 ± 0.05 , and $(V - I)_{-3.5,0} = 1.47$. These results correspond to a metallicity $[\text{Fe}/\text{H}] \approx -0.93$ (for S1) and $[\text{Fe}/\text{H}] \approx -1.31$ (for S2), and a distance $(m - M)_0 = 29.29$ (S1) and 29.22 (S2). The distance modulus of NGC 4631, based on the average results for two fields is $(m - M)_0 = 29.26 \pm 0.04$, that correspond to a distance $D = 7.11 \pm 0.13$ Mpc. Roughly selecting stars around the neighboring NGC 4627, we found the TRGB edge of their luminosity function at $I_{\text{TRGB},0} = 25.12$ and the RGB colour of $(V - I)_{-3.5,0} = 1.38$. The derived distance of NGC 4627 $(m - M)_0 = 29.13$ ($D = 6.70 \pm 0.15$ Mpc) is less certain than the distance estimation of NGC 4631, due to the small star number counts and unclear contamination by the NGC 4631 stars, but it confirms their proximity to each other.

3.2.4. NGC 5023

The I – *band* luminosity function of RGB stars in the outer area of IC 5023 (Fig. 4), has a discontinuity at $I_{\text{TRGB},0} = 24.95 \pm 0.05$ corresponding to the TRGB edge. We used the median colour between $I_0 = 25^m 3$ and $I_0 = 25^m 6$ to determine $(V - I)_{-3.5,0}$, is $1^m 35$. These results correspond to a metallicity $[\text{Fe}/\text{H}] \approx -1.7$, and a distance $(m - M)_0 = 28.94$ ($D = 6.14 \pm 0.15$ Mpc).

3.2.5. Comparison to previous distance estimations

In the context of distance verification, it is a valuable opportunity to compare our TRGB distances estimations with a results of other methods. We also list distances calculated by Seth et al. (2005a) as $D_{\text{SDJ}2005}$, who used the similar TRGB method from HST data.

There are three published distance estimations for IC 2233: 7.7 Mpc (Rossa et al. 2004), 6.9 Mpc (Wilcots & Prescott 2004), and 10.6 Mpc (Tully 1988). Our distance measurement, $D = 10.4$ Mpc, does agree well with the Tully (1988) determination, but significantly differs from two other results.

For IC 5052, we found the following previous estimations: A distance of 6.0 Mpc reported by Seth et al. (2005a), 6.3 Mpc by Karachentsev et al. (2004), 7.9 Mpc by Rossa et al. (2004), 5.9 Mpc (Ryan-Weber et al. 2003), and 9.2 Mpc (Becker et al. 1988). Our value is $D = 5.6$ Mpc.

While our distance for NGC 4631, $D = 7.1$ Mpc, is close to the Rand & van der Hulst (1993) measurement of 7.5 Mpc and 7.6 Mpc by Seth et al. (2005a), it significantly disagrees with the estimation of 5.3 Mpc by Sofue & Handa (1990).

There are a few distance estimations for NGC 5023. van der Kruit & Searle (1982) accepted a distance of 8 Mpc based on its redshift and $H_0 = 75 \text{ km s}^{-1} \text{ Mpc}^{-1}$. Distances of 5.6 Mpc (Bottinelli et al. 1985) and 4.8 Mpc (Swaters et al. 2002) were calculated using the Tully-Fisher relation. A brightest star method measured by Sharina et al. (1999) gives $D = 5.4$ Mpc. Our TRGB distance is 6.14 Mpc, that is in an agreement with $D_{\text{SDJ2005}} = 6.61$ by Seth et al. (2005a).

4. Stellar spatial distributions

The regions outlined in Fig. 2 and 3 indicate the regions of the AGB, “blue plum” and RGB stars used for the analysis of their extraplanar distribution. Similarly to our previous studies of the outer stellar surroundings of the disk galaxies (Drozdovsky et al. 2003; Tikhonov et al. 2005; Tikhonov & Galazutdinova 2005), we apply the following method. Using colour-magnitude diagrams, we separate different stellar populations and analyze their spatial distribution. By sorting stars on the different groups according to their life expectancies, we assign probable membership of stars to the different galaxy components. The measurements of the stellar number density perpendicular to the galaxy plane and search for the truncation radius (edge) of the thin and thick disks allow us to trace farther a presence of stellar halo. Unless otherwise stated, it is assumed that stellar thick disk and halo are close to axially symmetric, allowing us to extrapolate the spatial distribution from mapping only a part of the galaxy. Forthcoming, we will examine the case of two neighboring galaxies, where strong tidal forces might cause an asymmetry of the stellar structures.

The extraplanar distribution of the stars (see Fig. 5), shows a decline toward the mid-plane of the thin disks, due to the increase of stellar crowding and concentration of dust, rapid growth to some extraplanar distance, followed by steady exponential decline. The radially truncated exponential disks are routinely observed in the disk-dominated edge-on galaxies, relying on the surface photometry (e.g., de Grijs & van der Kruit 1996; de Grijs et al. 2001; Pohlen et al. 2004) and stellar number counts (Tikhonov & Galazutdinova 2005). The surface number density profiles such as ones presented in Fig. 5 show, that distribution of different stellar populations has quite different scale-lengths and truncation radii.

Fig. 5. The surface number density distribution (SN) of RGB (*filled squares*), AGB (*dots*) and blue stars (*empty squares*) along the extraplanar Z-axis.

The young blue stars reside mostly in the thin disk, that has a large concentration of dust. However, the majority of these stars are bright enough to be detected even near the mid-plane of a thin disk, and therefore they do not show the same drop-out as less luminous evolved stars (AGB and RGB).

4.1. IC 2233

The intermediate-age AGB stars are generally more extended than blue stars and their extraplanar distribution roughly follows the exponential law. At extraplanar distance of $Z \simeq 1.6$ Mpc their number density drops to almost zero. The underdensity of the AGB stars make it difficult to obtain representative information on their outermost extend. In our previous studies, we found that in galaxies with larger sample of AGB stars, such as in NGC 891, there are two gradients of the AGB stars distribution: the steep decline of the inner AGB components until 6 kpc, and the shallow decline of the outer AGB component traced at least up to 11 kpc above the mid-plane (Tikhonov & Galazutdinova 2005). The most numerous among detected, RGB stars have the shallowest of all stellar number density gradients. The drop of their number near the galactic mid-plane is due to their low luminosity. At the extraplanar distance of $Z = 1.9$ kpc the RGB stars show a break in the exponential decline of their surface density, that likely corresponds to

a vertical (extraplanar) edge of the thick disk. Farther above the thick disk, a density of the RGB stars declines with a shallower slope. By fitting the exponential law, we extrapolated stellar halo out to $Z = 4.8$ kpc. Unless there is an additional outermost stellar component not covered by the ACS/WFC field, the relatively small extent of the stellar halo in comparison with apparent large axis length (planar extent) indicates that stellar halo might be represented by oblate ellipsoid.

Stil & Israel (2002) believed that galaxies IC 2233 and NGC 2537 are a physical pair. However, we did not find any apparent tidal deformations of the IC 2233 thick disk, as we detected in the interacting NGC 4631. Therefore, we assume an axial symmetry for the disk and halo components of IC 2233.

It is valuable to compare the extraplanar size of the outermost stellar and gaseous structures of IC 2233. It is generally assumed that the size of the neutral hydrogen envelopes of the disk-dominated galaxies is several times larger than the stellar halos (e.g., Martin 1998; Swaters et al. 2002). Rescaled to our estimation of the IC 2233 distance, $D = 10.4$ Mpc, the extraplanar height of the H_I envelope is $Z(\text{H}_\text{I}) = 2.4$ kpc according to measurements of Stil & Israel (2002), or 6.1 kpc according to Wilcots & Prescott (2004). We detected the edge of the IC 2233 thick disk at extraplanar distance of 3.8 kpc, while its stellar halo is traced as far as 9.6 kpc. Note that the extraplanar emission-line gas was traced out to ~ 1 kpc from the IC 2233 mid-plane (Miller & Veilleux 2003).

4.2. IC 5052

Similarly to IC 2233, the young blue stars of IC 5052 are concentrated in the thin disk, that truncated at ~ 1 kpc above the mid-plane. The intermediate-age AGB stars are confined in both the thin and thick disks and can be seen out to $Z = 1.6$ kpc. The old/intermediate-age RGB stars reveal break in their surface density at $Z = 1.9$ kpc, but extend farther with smaller surface density gradient tracing a stellar halo. The extrapolated vertical size of the halo is $Z \simeq 4.0$ kpc.

There is a reported detection of a bright H_I-halo and extended emission (Rossa & Dettmar 2003), but the exact size is unknown. In the presented H_I column density contours (Ryan-Weber et al. 2003), the IC 5052 vertical structure is seen at least until $Z = 3.2$ kpc, but there are also indication on more extended hydrogen filaments.

4.3. NGC 4631/4627

Since one of the ACS/WFC fields (S1) covers partly the circumnuclear area of NGC 4631 while second one (S2) are well off-center along the disk-plane, we can easily discern the bulge stars from the disk and halo ones (see Fig. 1). The distribution of stars detected in the field S1 are symmetric, and show a significant extent as for the young blue stars (truncation height $Z \simeq 2.0$ kpc), intermediate-age AGB stars ($Z \simeq 4.0$ kpc), and RGB stars, which spread farther than the S1 field borders.

The surface density profile of stars detected in the S2 field show quite different distribution. Only profile of blue stars is symmetric relatively to the mid-plane, while AGB and RGB stars show asymmetric breaks at opposite sides of galactic plane: the north side is clearly truncated at smaller extraplanar distance than the south one. For the AGB stars the South-to-North sides asymmetry of this break is $Z_{\text{South}}/Z_{\text{North}}(\text{AGB}) = 2.8 \div 4.0$ kpc, and for the RGB stars $Z_{\text{South}}/Z_{\text{North}}(\text{RGB}) = 3.1 \div > 4.5$ kpc.

The peculiar distribution of the evolved AGB and RGB stars can be explained by different possibilities:

- i)* The interaction between NGC 4631 and NGC 4627 distorted closest (Northern) side of the thick disk and halo, that resulted in their spread out toward North part from galaxy plane. The spatial stretch of stellar structures yielded to the diminishing of their surface density. Certainly, some of the outermost stars in that area might actually belong to NGC 4627. Another difficulty of this model is to explain the high-degree symmetry of the distribution of blue stars relatively to the galaxy plane, as it was found in both of the studied fields, S1 and S2.
- ii)* The asymmetry in the distribution of evolved stars is purely due to the mixing of the NGC 4627 stars with NGC 4631. This model is not supported by the data, since the surface overdensity is detected toward the opposite (Southern) side across the NGC 4631 plane.
- iii)* The asymmetry in detection of the AGB stars of NGC 4631 is due to the presence of the foreground dust clouds in NGC 4627, that significantly dim light of the NGC 4631 stars, shifting them below the magnitude of the TRGB. This mechanism might yields to the observable undercounting of AGB stars by 2.3 times, and requires an average interstellar extinction of about one magnitude in *I*-band, that is possible for ~ 1 kpc extraplanar distance (Golla et al. 1996; Martin & Kern 2001). The RGB stars are more spread out and thus less affected by dust extinction. Therefore their South-to-North surface densities differ less (the ratio is $3 \div 2$). This model is supported by the H I-feature (spur 4), plausibly associated with NGC 4627 and apparent on the radio-images (Rand & van der Hulst 1993; Rand 1994).

We estimated the outermost vertical extension of the NGC 4631 stellar halo as $\approx 8 \div 10$ kpc. Interestingly, from the spectroscopic observations Martin & Kern (2001) have detected the extraplanar emission line gas around NGC 4631 out to $Z \simeq 7$ kpc.

4.4. NGC 5023

As in the case of IC 2233 and IC 5052, the stellar surface density of NGC 5023 stars are symmetric relatively to a disk plane within the observed field. The young blue stars are prominent but confined to the narrow plane ($Z = \pm 0.8$ kpc) of the galaxy thin disk. The extraplanar size of the disk-like structure of AGB stars is 1.3 kpc, while thick disk of the RGB stars show break at $Z = 1.6$ kpc. The halo are well traced above by RGB stars until $Z = 3.2$ kpc. NGC 5023 is the most flattened among analyzed edge-on galaxies with length-to-height ratio of $a/b = 9.3$ (NED). Interestingly, the stellar halo of this galaxy indicate also of the largest flatness. Does it

indicate the rotation of the halo? The corrugation of the NGC 5023 disk have been reported by Florido et al. (1991), similarly to the disk of the Milky Way. The H_I-disk of the NGC 5023 show a sharp edge at $Z = 1.8$ kpc, while some of the hydrogen filaments are seen at larger distances (Swaters et al. 2002).

5. Extraplanar colour gradients of the RGB stars

Metal abundances act as a tracer to the conjoint action of star formation and dynamical mixing of stars and gas within a galaxy. Therefore spatial abundance variations are among the most important parameters in any theory of galactic chemodynamical evolution. The majority of the investigations concentrated predominantly on the radial (in-plane) abundance gradients in the galactic disks, which have been established in the Galaxy and other nearby disk galaxies based on the spectroscopy of a variety (mostly of young) objects such as stellar clusters, H_{II} regions, planetary nebulae, and brightest stars (e.g., Shaver et al. 1983; Friel & Janes 1991; Rolleston et al. 2000; Márquez et al. 2002; Andrievsky et al. 2002). Edge-on galaxies provide an opportunity to explore the abundance gradient as a function of extraplanar height, that ensure minimal contamination by stars belonging to the dominant galactic disk component. However, only a few edge-on galaxies are close enough to perform metallicity measurements from the spectrum of evolved stellar populations due to their low luminosity (Reitzel & Guhathakurta 2002). The idea to use the $(V - I)$ colour of the RGB stars comes from its much greater sensitivity to metallicity than it has to age, making the mean RGB colour a good stellar metallicity indicator, although there is some degeneracy (Lee et al. 1993). The method is based on the statistical approach and its accuracy depends on the quality of the photometric data as well as on the number of detected RGB stars (including the source confusion—Galactic red dwarfs, etc...). The advantage of this method is that red giants can be situated at relatively large galactocentric distances, where surface brightness is very low and spectral methods are below the sensitivity limits.²

The number density of RGB stars varies several orders of magnitude across the extraplanar space. To include statistically significant data, we track colour changes of RGB stars located in three major areas: the equatorial (thin disk) zone, thick disk and halo. We consider only two galaxies for this study, NGC 5023 and IC 5052. NGC 4631 shows the apparent distortion of its disk, and make it difficult to separate stars belonging to different spatial substructures. IC 2233 is too distant to collect enough stars for the reliable statistical study.

Extraplanar colour distribution of RGB stars are similar in NGC 5023 and IC 5052 (see Fig. 6) and characterized by weak negative median $(V - I)$ gradient out to the “halo” area.

² Note, that the metallicity gradients of young and evolved stars reflects different structures, and are the subject of the different star forming and kinematic effects: *i* These estimations deal with different (spatial?) substructures – thick and thin disks. *ii* The metallicity of young stars reflects rather the SFR and CEL, while the distribution of old stars are more depends on the effectiveness of the process of stellar mixing. We consider here only the metallicity of the upper (brightest) part of the RGB (i.e. intermediate-age/old stellar populations).

Fig. 6. The distribution of the $(V - I)$ color of the RGB stars from 0.3 to 0.7 mag below the tip of the RGB for three extraplanar zones: thin and thick disks (*solid lines*) and halo (*dotted line*). The similar morphology gradient in the RGB is visible in both of the edge-on galaxies, NGC 5023 and IC 5052: the red RGB stars are more concentrated to the disk plane, while outermost extraplanar stars are systematically bluer.

Zero or slightly negative vertical colour gradient have also been found in some other previously studied edge-on disk galaxies, such as NGC 55 and NGC 4244 (Tikhonov et al. 2005; Tikhonov & Galazutdinova 2005). There is no apparent changes in colour gradient within the thick disk area based on our measurements. Mould (2005) found the zero or slightly positive vertical colour gradients for the RGB stars in the thick disks of four others local edge-on galaxies, but no data was available for the $z > 2$ kpc area of these galaxies. Based on the similar HST data, Seth et al. (2005b) confirmed that extraplanar stars show little or no colour gradient.

Note, that no correction has been made for interstellar reddening, that might mostly affect the colours of the thin disk stars. Additionally due to the crowding, the sample of objects within a few hundreds parsecs of the disk mid-plane is likely dominated by the outer-disk stars with large

Fig. 7. A scaled 3-D representation of the stellar components of a typical spiral galaxy and results of their projection as a stellar number density for a face-on (*bottom plot*) and edge-on (*right*) galaxy.

galactocentric radii. The lack of the inner-disk RGB stars, as well as age-metallicity bias might significantly impact the cumulative colour distribution. Thus the lack of strong colour gradient do not ruled out the systematic chemical changes of RGB stars perpendicular to a disk plane, as well as star to star variations in elemental abundance ratios. Even the outermost “halo” RGB stars apparently show a large range of colours, indicating that extraplanar areas have experienced a complicated star formation history with various self-enrichment processes.

6. Model of the stellar structures of a disk galaxy

Comparing the inferred parameters for the thin & thick disk and halo with our and other published results, we compose a scale 3-D model of the stellar structures of a typical disk galaxy (Fig. 7). This model relies on the star number counts in the low-inclination, M 81 and NGC 300, and eight high-inclination disk galaxies, NGC 55, NGC 891, NGC 4144, NGC 4244, NGC 4363, NGC 5023, IC 2233, IC 5052 (Tikhonov et al. 2005; Tikhonov & Galazutdinova 2005, this paper). Now we have new results of stellar photometry of four disk galaxies: NGC 1311, UGC 1281, UGC 8760 and IC 1959 that to support this model of the stellar structure. While our primary goal in this work is to constrain the spatial geometry of the spiral galaxies, we would like to note that massive irregular galaxies, such as IC 10 (Drozdovsky et al. 2003) and M 82 (Tikhonov 2005), show all kinds of the stellar structures, including thick disk and halo. The spatial distribution of stars along and perpendicular to a disk galaxy plane are alike. The young blue stars are mostly confined to the thin disk of the galaxy, while elder stars are more spread out with oldest stars are traced outermost.

Table 2. Properties of Galaxies

Name	R.A.(2000.0)	DEC(2000.0)	V_h	$a \times b$	B_t	B_t^0	Type	A_v	i	$m - M$	M_B
IC2233	08 ^h 13 ^m 58 ^s .91	+45°44'31".7	565	5.2×0.6	13.07	11.70	SB(s)d:sp	0.171	90	30.09	-18.39
IC5052	20 ^h 52 ^m 01 ^s .63	-69°11'35".9	598	5.9×0.8	11.16	10.52	SBd:sp	0.168	90	28.75	-18.23
NGC4631	12 ^h 42 ^m 08 ^s .01	+32°32'29".4	606	15.5×2.7	9.75	8.61	SB(s)d	0.056	90	29.26	-20.65
NGC5023	13 ^h 12 ^m 12 ^s .60	+44°02'28".4	407	7.3×0.8	12.85	11.59	Scd	0.060	90	28.94	-17.35

The Galactic extinction correction is by Schlegel et al. (1998).

The inclination is taken from LEDA.

The value of ($m - M$) is from this paper.

7. Discussion

Relying on the star number counts in the disk galaxies IC 2233, IC 5052, NGC 4631 and NGC 5023, we examine the extraplanar spatial distribution of young and evolved stars in their disks and halos. These edge-on disk galaxies show the similar morphological properties, thin and thick disks and halo, but relative sizes of these structures are different in each galaxy. Combining this work with results obtained for other four large edge-on disk galaxies Tikhonov et al. (2005); Tikhonov (2005), we suggest that most of the massive disk galaxies have not only a thick disk but also an extended halo, consisting mainly of evolved stars.

The stellar number density of the halo at the truncation radius (break) of the thick disk varies a lot, and plausibly correlate with overall flatness of a disk galaxy. The ratio of the halo-to-thick disk size is relatively constant, $R_{\text{halo}}/R_{\text{thickdisk}} = 2.5 \pm 0.5$. It might reflect the overall rotation of the galaxy, including flatten stellar halo.

Noteworthy the significant contrast between stellar structures of two nearest giant spiral galaxies, the Milky Way and M 31, the only systems there possible to measure the kinematics and chemical properties of individual stars. While both of the “sister” galaxies are about the same baryonic-plus-dark masses, their stellar disks and halo differ significantly. The outer second disk-like stellar structure of M 31 are 3-4 times more extended than in our Galaxy and dominate over the halo stars at least out to a de-projected galactocentric radii of about 40 kpc (e.g., Worley et al. 2005; Ibata et al. 2005). The significant difference in the properties of the outer stellar populations of the nearby disk galaxies, such as the Milky Way, M 31, and others (including our dataset) plausibly suggest that the final morphology of a galaxy is extremely sensitive to the details of the satellite accretion history, as well as peculiarities of the star formation and feedback.

Such unique populations as bulge, thin and thick disks, and halo have likely formed by different mechanisms, especially considering the differences in ages and metallicities. The thick disk and halo may cast light on the most ancient structure formation, so being extremely important

for the understanding of early history of galaxy formation and evolution. If stellar halo have been formed prior to the thick disk (see a recent review of various formation scenarios for the stellar halo by Wyse 2003), the later should show both the characteristics age and metallicity profile of a posthalo epoch of star formation 6-12 Gyr ago and differ significantly from the halo (Mould 2005). The addition of results from photometry of more evolved stars (e.g., Horizontal Branch and old Main-Sequence Turn-Off stars), as well as from kinematic and chemistry of resolved stars are required to refine various formation scenarios.

8. Summary

On the basis of the star count method, we have analyzed extraplanar stellar structures in four large high-inclination galaxies. The main results can be summarized as follows:

- The extended stellar thick disks and halos have been detected in IC 2233, IC 5052, NGC 4631 NGC 5023.
- There are clear differences between surface density gradients of evolved stellar populations assigned to the thick disk and halo of these disk galaxies, which allowed us to detect the edge of the thick disk. The extraplanar distribution of the outermost stars indicate that stellar halo is flattened along the extraplanar direction.
- Having a large, high quality photometry of the RGB stars allowed us to estimated the distances to the galaxies from the TRGB magnitude with high confidence. We determine a distance of 10.42 ± 0.38 Mpc for IC 2233, 5.62 ± 0.20 Mpc for IC 5052, 7.11 ± 0.13 Mpc for NGC 4631 (6.70 ± 0.15 for its satellite NGC 4627) and 6.14 ± 0.15 Mpc for NGC 5023.
- In NGC 4631, the revealed asymmetry of its stellar thick disk and halo, plausibly is an evidence of an past or ongoing interaction with NGC 4627.
- The stellar distribution of stellar populations of these four galaxies provide more confidence for the unified model of three-dimensional structure of large disk galaxies, and motivate follow-up spectroscopic study to constrain the kinematic characteristics of the stellar components.

Acknowledgements. This work has been financially supported by grant RFBR 03-02-16344. Data from the NASA/IPAC Extragalactic Database have been used.

References

Abadi, M. G., Navarro, J. F., Steinmetz, M., & Eke, V. R. 2003, *ApJ*, 597, 21
 Andrievsky, S. M., Kovtyukh, V. V., Luck, R. E., Lépine, J. R. D., et al. 2002, *A&A*, 381, 32
 Arp, H. 1966, *ApJS*, 14, 1
 Becker, R., Mebold, U., Reif, K., & van Woerden, H. 1988, *A&A*, 203, 21
 Bellazzini, M., Ferraro, F. R., & Pancino, E. 2001, *ApJ*, 556, 635
 Bettoni, D. & Buson, L. 1987, *A&AS*, 67, 341

Bottinelli, L., Gouguenheim, L., Paturel, G., & de Vaucouleurs, G. 1985, *A&AS*, 59, 43

Brewer, M. & Carney, B. W. 2004, *PASA*, 21, 134

Brook, C., Kawata, D., Gibson, B., & Freeman, K. 2004, *ApJ*, 612, 894

Brown, T. M., Ferguson, H. C., Smith, E., Kimble, R. A., et al. 2003, *ApJ*, 592, 17

Bullock, J. S. & Johnson, K. V. 2005, *ApJ*, 635, 931

Cardelli, J. A., Clayton, G. C., & Mathis, J. S. 1989, *ApJ*, 345, 245

Chiba, M. & Beers, T. 2000, *AJ*, 119, 2843

Cuillandre, J.-C., Lequeux, J., & Loinard, L. 1999, in IAU Symposium, 185

Dalcanton, J. & Bernstein, R. 2002, *AJ*, 124, 1328

de Grijs, R., Kregel, M., & Wesson, K. H. 2001, *MNRAS*, 324, 1074

de Grijs, R. & van der Kruit, P. C. 1996, *A&AS*, 117, 19

Drozdovsky, I. O., Tikhonov, N. A., & Schulte-Ladbeck, R. E. 2003, in STScI Symposium "The Local Group" May 2003, 25

Ferguson, A. M. N., Irwin, M. J., Ibata, R. A., Lewis, G. F., & Tanvir, N. R. 2002, *AJ*, 124, 1452

Florido, E., Battaner, E., Prieto, M., Mediavilla, E., & Sanchez-Saavedra, M. L. 1991, *MNRAS*, 251, 193

Friel, E. D. & Janes, A. 1991, *A&A*, 251, 193

Fry, A., Morrison, H., Harding, P., & Boroson, T. A. 1999, *AJ*, 118, 1209

Gilmore, G. & Reid, N. 1983, *MNRAS*, 202, 1025

Gnedin, O. Y. 2003, *ApJ*, 589, 752

Golla, G., Dettmar, R.-J., & Domgorgen, H. 1996, *A&A*, 313, 439

Goudfrooij, P., Gorgas, J., & Jablonka, P. 1999, *Ap&SS*, 269, 109

Holmberg, E. 1937, *Annals of the Observ. of Lund*, 6, 1

Holtzman, J. A., Burrows, C. J., Casertano, S., Hester, J. J., et al. 1995, *PASP*, 107, 1065

Hoopes, C. G., Walterbos, R. A. M., & Rand, R. J. 1999, *ApJ*, 522, 669

Howk, J. C. & Savage, B. D. 1999, in *The Physics and Chemistry of the Interstellar Medium*, Eds.: V. Ossenkopf, J. Stutzki, and G. Winnewisser, 38, astro-ph/9810438

Ibata, R., Chapman, S., Ferguson, A. M. N., et al. 2005, *ApJ*, 634, 287

Karachentsev, I. D., Karachentseva, V. E., Huchtmeier, W. K., & Makarov, D. I. 2004, *AJ*, 127, 2031

Keppel, J. W., Dettmar, R., Gallagher, J. S., & Roberts, M. S. 1991, *ApJ*, 374, 507

Koekemoer, A. M., Fruchter, A. S., Hook, R. N., & Hack, W. 2002, in *The 2002 HST Calibration Workshop*, Ed. by Santiago Arribas, Anton Koekemoer, and Brad Whitmore. Baltimore: STScI, 339

Kroupa, P. 2002, *MNRAS*, 330, 707

Lee, M., Freedman, W., & Madore, B. 1993, *AJ*, 417, 553

Márquez, I., Masegosa, J., Moles, M., et al. 2002, *A&A*, 393, 389

Martin, C. & Kern, B. 2001, *ApJ*, 555, 258

Martin, M. 1998, *A&AS*, 131, 77

McWilliam, A. & Smecker-Hane, T. A. 2005, *ASPC*, 336, 221

Miller, S. & Veilleux, S. 2003, *ApJ*, 592, 79

Mould, J. 2005, *AJ*, 129, 698

Pavlovsky, C. et al. 2005, *ACS Data Handbook*, Tech. Rep. Version 4.0, Baltimore: STScI

Pohlen, M., Balcells, M., Lüticke, R., & Dettmar, R.-J. 2004, *A&A*, 422, 465

Prochaska, J., Naumov, S., Carney, B. W., McWilliam, A., & Wolfe, A. M. 2000, *AJ*, 120, 2513

Rand, R. 1994, *A&A*, 285, 833

Rand, R. & van der Hulst, J. 1993, *AJ*, 105, 2098

Reitzel, D. B. & Guhathakurta, P. 2002, *AJ*, 124, 234

Rolleston, W. R. J., Smartt, S. J., Dufton, P. L., & Ryans, R. S. I. 2000, *A&A*, 363, 537

Rossa, J., Dettmar, R., Walterbos, R. A. M., & Norman, C. A. 2004, *AJ*, 128, 674

Rossa, J. & Dettmar, R.-J. 2003, *A&A*, 406, 493

Rowe, J., Richer, H., Brewer, J., & Grabtree, D. 2005, *AJ*, 129, 729

Ryan-Weber, E., Webster, R., & Staveley-Smith, L. 2003, *MNRAS*, 343, 1185

Sackett, P. D. 1999, in *Astronomical Society of the Pacific Conference Series*, 393

Sarajedini, A. & Van Duyne, J. 2001, *AJ*, 122, 2444

Savage, B. D., Sembach, K. R., Wakker, B. P., Richter, P., et al. 2003, *ApJS*, 146, 125

Schlegel, D., Finkbeiner, D., & Davis, M. 1998, *ApJ*, 500, 525

Seth, A. C., Dalcanton, J. J., & de Jong, R. S. 2005a, *AJ*, 129, 1331

Seth, A. C., Dalcanton, J. J., & de Jong, R. S. 2005b, *A&AS*, 207, 8705

Sharina, M. E., Karachentsev, I. D., & Tikhonov, N. A. 1999, *Astronomy Letters*, 25, 322

Shaver, P. A., McGee, R. X., Newton, L. M., Danks, A. C., & Pottasch, S. R. 1983, *MNRAS*, 204, 53

Smecker-Hane, T., McWilliam, A., & Ibata, R. 1998, *BAAS*, 30, 916

Sofue, Y. & Handa, T. 1990, *PASJ*, 42, 745

Stetson, P. 1994, *Users Manual DAOPHOT II*, Tech. rep., Dominion Astrophysical Observatory

Stil, J. & Israel, F. 2002, *A&A*, 389, 29

Swaters, R. A., van Albada, T. S., van der Hulst, J. M., & Sancisi, R. 2002, *A&A*, 390, 829

Tüllmann, R., Rosa, M. R., Elwert, T., Bomans, D. J., et al. 2003, *A&A*, 412, 69

Tiede, G., Sarajedini, A., & Barker, M. 2004, *AJ*, 128, 224

Tikhonov, N. 2005, *Astron.Let.*, submitted

Tikhonov, N. A. & Galazutdinova, O. A. 2005, *Astrophysics*, 48, 221, paper II

Tikhonov, N. A., Galazutdinova, O. A., & Drozdovsky, I. O. 2005, *A&A*, 431, 127, paper I

Tully, R. B. 1988, *Nearby Galaxies Catalog* (Cambridge: Cambridge Univ. Press)

Vallenari, A., Bertelli, G., & Schmidtbreick, L. 2000, *A&A*, 361, 73

van der Kruit, P. C. & Searle, L. 1982, *A&A*, 110, 61

van der Marel, R. 2002, in “The shapes of galaxies and their dark matter halos”, New Haven, Connecticut, USA, 28-30 May 2001. Edited by Priyamvada Natarajan., 202

Venn, K. A., Irwin, M., Shetrone, M. D., Tout, C. A., et al. 2004, *AJ*, 128, 1177

Wilcots, E. & Prescott, M. 2004, AJ, 127, 1900

Williams, B. F. 2002, MNRAS, 331, 293

Worthey, G., Espana, A., MacArthur, L. A., & Courteau, S. 2005, ApJ, 631, 820

Wyse, R. 2003, in STScI Symposium "The Local Group" May 2003, ed. M. Livio, astro-ph/0402636

Zheng, Z., Shang, Z., Su, H., et al. 1999, AJ, 117, 2757

Zibetti, S. & Ferguson, A. M. N. 2004, MNRAS, 352, L6

Zibetti, S., White, S. D. M., & Brinkmann, J. 2004, MNRAS, 347, 556

Zucker, D. B., Kniazev, A. Y., Bell, E. F., et al. 2004, ApJ, 612, L117

List of Objects

- ‘IC 2233’ on page 1
- ‘IC 5052’ on page 1
- ‘NGC 4631’ on page 1
- ‘NGC 4627’ on page 1
- ‘NGC 5023’ on page 1
- ‘M 81’ on page 4
- ‘NGC 300’ on page 4
- ‘NGC 55’ on page 4
- ‘NGC 891’ on page 4
- ‘NGC 4144’ on page 4
- ‘NGC 4244’ on page 4
- ‘IC 10’ on page 4
- ‘NGC 1311’ on page 17
- ‘UGC 1281’ on page 17
- ‘UGC 8760’ on page 17
- ‘IC 1959’ on page 17